DOI: 10.1002/ejic.201000959

A Dinuclear Gold(I)–Silver(I) Derivative of 2-Cyclopentylidene-2-sulfanylacetic Acid and Related Complexes: Synthesis, Crystal Structures, Properties and Antitumor Activity

Elena Barreiro,[a] José S. Casas,[a] María D. Couce,[b] Antonio Laguna,*[c] José M. López-de-Luzuriaga,[d] Miguel Monge,[d] Agustin Sánchez,[a] José Sordo,*[a] José M. Varela,[a] and Ezequiel M. Vázquez López[b]

Keywords: Gold / Silver / Sulfanylcarboxylic acids / NMR spectroscopy / Luminescence / Cytotoxicity

The dinuclear complex [AgAu(PPh_3)$_2$cpa] (H_2cpa = 2-cyclopentylidene-2-sulfanylacetic acid) was prepared by treating the precursor [Au(PPh_3)(Hcpa)] with Ag(PPh_3)NO_3. The complex was characterised by spectroscopic methods (IR; ^{1}H, ^{13}C, ^{31}P NMR) and mass spectrometry, and the structure was solved by a single-crystal X-ray diffraction study. Luminescence and theoretical studies were carried out, and the antitumor activity was studied in vitro against HeLa-229, A2780 and A2780cis cell lines. The related gold(I)–gold(I), [(AuPPh_3)$_2$cpa], and silver(I)–silver(I), [(AgPPh_3)$_2$cpa], compounds were also prepared and studied in the solid state and in solution.

Introduction

Gold and gold-containing compounds have been used in medicine for centuries and, as a result of their potential usefulness, such compounds have been widely investigated and knowledge of their mechanism of action is increasing.[1–4] As our understanding of these compounds has increased, new and interesting properties have been identified and studied.

One such property is luminescence, which has the potential to enable investigations into the intracellular distribution of gold complexes, as highlighted recently.[5] This property was identified in compounds in which a gold–gold (aurophilic) interaction[6,7] is present and also in compounds where metal centres other than gold can establish gold–metal (metallophilic) interactions.[8,9] These interactions have been studied in compounds in which the two metals have a direct interaction (i.e. without other atoms being involved) or, alternatively, where the interaction is supported by ligand atoms – situations that give rise to unsupported or supported interactions, respectively. In the specific case of gold(I)–silver(I) interactions, several polymeric structures with different nuclearities have been identified (vide infra), but the number of dinuclear complexes studied is limited.[8]

Interesting from a biological point of view are (thiolato)-gold(I) compounds of the type [Au(PR_3)(SR)],[10] the luminescent properties of which have recently been reviewed.[11] The gold–gold interaction in these compounds, where present, is unsupported, and Au atoms from neighbouring [Au(PR_3)(SR)] molecules are directly bonded to give supramolecular chains.

We recently described dinuclear (thiolato)gold(I) compounds of the type [(AuPPh_3)$_2$(SR)] [H_2SR = (3-aryl-)2-sulfanylpropenoic acids], in which two Au atoms form an interaction which is supported by an S atom bridging the two metal centres.[12] These compounds have interesting in vitro antitumor properties[13] and were prepared by treating gold(I) precursors of the type [Au(PPh_3)(HSR)] with Au(PPh_3)Cl.

Bearing in mind the limited number of dinuclear gold(I)–silver(I) compounds studied to date[8] and the lack of compounds of this type that are S-supported, we treated a similar precursor with a silver(I) compound to obtain an equivalent dinuclear gold(I)–silver(I) compound in which the S atom, which supports the interaction, comes from the doubly deprotonated 2-cyclopentylidene-2-sulfanylacetic acid (H_2cpa) ligand.

The preparation, structural characterisation, luminescence and theoretical studies for this compound, [AgAu(PPh_3)$_2$cpa], are described, and the in vitro antitu-

[a] Departamento de Química Inorgánica, Facultade de Farmacia, Universidade de Santiago de Compostela, 15782 Santiago de Compostela, Spain
Fax: +34-981-547-102
E-mail: jose.sordo@usc.es
[b] Departamento de Química Inorgánica, Facultade de Química, Universidade de Vigo, 36310 Vigo, Spain
[c] Departamento de Química Inorgánica, Instituto de Ciencia de Materiales de Aragón, Universidad de Zaragoza – CSIC, 50009 Zaragoza, Spain
E-mail: alaguna@unizar.es
[d] Departamento de Química, Universidad de La Rioja, Grupo de Síntesis Química de La Rioja, UA-CSIC, Complejo Científico-Tecnológico, 26004 Logroño, Spain

Supporting information for this article is available on the WWW under http://dx.doi.org/10.1002/ejic.201000959.

mor activity is also reported. The equivalent gold(I)–gold(I), [$(AuPPh_3)_2$cpa], and silver(I)–silver(I), [$(AgPPh_3)_2$-cpa], compounds were also prepared and structurally identified for comparative purposes.

Results and Discussion

Synthesis and Structural Characterisation

A summary of the reactions that led to the complexes described in this paper is provided in Scheme 1. As can be seen, [$(AuPPh_3)_2$cpa] (**2**) was synthesised from the reaction between [$Au(PPh_3)$(Hcpa)] (**1**), $Au(PPh_3)Cl$ and NaOH in methanol/water, as described previously for other dinuclear (sulfanylcarboxylato)(triphenylphosphane)gold(I) complexes.[12] In an effort to confirm the incorporation of Ag into **1**, the reaction of this compound with $Ag(PPh_3)NO_3$ was monitored by ESI/MS. The formation of a complex containing Ag and Au was confirmed by the presence, in the mass spectrum, of a peak at m/z = 986.0 resulting from $[AgAu(PPh_3)_2cpa]^+$. The presence of both metals in the isolated solid **3** was confirmed by X-ray fluorescence and chemical analysis. Heterogeneous conditions were used to obtain [$(AgPPh_3)_2$cpa] (**4**), as described previously for other sulfanylsilver(I) complexes containing triphenylphosphane,[14,15] but in this case $Ag(PPh_3)NO_3$ was used directly instead of silver nitrate and triphenylphosphane. The complexes are soluble in MeOH, EtOH, acetone, DMSO and $CHCl_3$ but are insoluble in water and Et_2O.

The IR spectrum of **1**, in contrast to that of uncoordinated H_2cpa, does not contain the ν(SH) band at 2578 cm^{-1}, thus confirming the deprotonation of the SH group. The COOH bands (1659 vs, 1425 vs, 1283 vs) are only shifted slightly when compared with those in uncoordinated H_2cpa, which shows that this group is not deprotonated. These latter bands in the IR spectra of **2** and **3** are absent and are replaced by a strong band close to 1570 cm^{-1}, which can be assigned to the $\nu_{asym}(COO^-)$ vibration of the carboxylato group. This band appears at 1534 cm^{-1} in **4**. As in **1**, the presence of the PPh_3 ligand in **2**, **3** and **4** is confirmed by the two strong bands close to 1430 and 1480 cm^{-1}.

The molecular structure of [$(AuPPh_3)_2$cpa] (**2**) is shown in Figure 1, and selected distances and angles for this compound are shown in Table 1 along with data for [$AgAu(PPh_3)_2$cpa]. The crystal of **2** contains dinuclear $(AuPPh_3)_2$cpa units. As shown in Figure 1, the two Au atoms in the unit, Au(1) and Au(2), have different coordination environments. Au(2) is bonded to the S atom of the deprotonated SH group of the ligand and to the P atom of PPh_3. In addition to these Au–P and Au–S bonds, Au(1) is

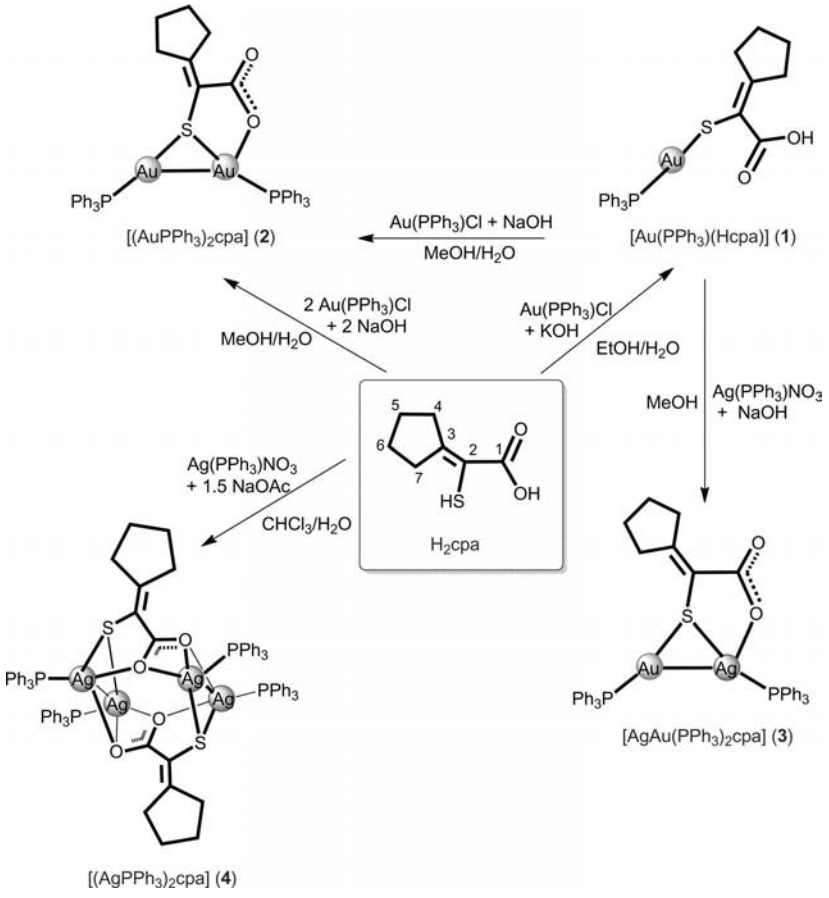

Scheme 1.

also coordinated to one of the O atoms of the carboxylato group. The Au(1)–O(11) bond length [2.537(12) Å], as well as the Au–S and Au–P bonds, is similar to those previously found in other dinuclear (sulfanylcarboxylato)gold(I) complexes.[12] As in the previously reported complexes the O-coordinated gold atom, Au(1), has longer Au–S and shorter Au–P bonds than the gold atom that is not O-coordinated. As far as the angles are concerned, the P–Au–S bond angle is significantly narrower for Au(1) than for Au(2). The Au(1)···Au(2) distance [3.0338(10) Å] is also close to those previously described for similar dinuclear Au complexes[12] and shorter than the sum of the van der Waals radii for this metal (3.70 Å).[16]

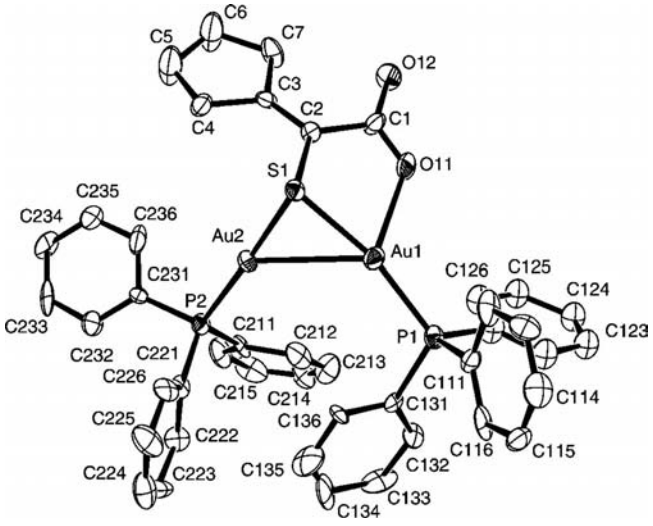

Figure 1. Structure of $[(AuPPh_3)_2(cpa)]$ (**2**) showing the numbering scheme. Ellipsoids are drawn at the 30% probability level.

The molecular structure of $[AgAu(PPh_3)_2cpa]$ (**3**) is shown in Figure 2 together with the numbering scheme, and selected distances and angles for this compound are listed in Table 1. The crystal contains $AgAu(PPh_3)_2cpa$ units in which the Au and Ag atoms have different coordination environments, as can be seen in Figure 2. Au(2) is bonded to the S atom of the deprotonated SH group of the ligand and to the P atom of PPh_3. Apart from the two similar bonds with S and P atoms, the Ag(1) atom is also bonded to one of the O atoms of the carboyxlato group of the cpa ligand. In this way, the structural arrangement in **3** is equivalent to that found in **2**, where Ag(1) in **3** plays the role of Au(1) in **2**.

The Ag(1)–O(11) bond length of 2.374(8) Å is similar to those found previously in (sulfanylcarboxylato)silver(I) complexes with different nuclearities[15] and, even though it is longer than equivalent distances found in other silver complexes,[17,18] it only exceeds the sum of the covalent radii of Ag and O (2.11 Å)[19] by 0.26 Å, thus showing a significant interaction. This interaction has a marked effect on the S–Ag(1)–P angle of 159.81(10)°, which is narrower than the S–Au(2)–P angle of 176.78(10)° in this complex, and is also narrower than the equivalent S–Au(1)–P angle in **2** of 166.21(15)° because of the weak M–O interaction in **2**.

Table 1. Selected interatomic distances [Å] and angles [°] for complexes $[(AuPPh_3)_2(cpa)]$ (**2**) and $[AgAu(PPh_3)_2(cpa)]$ (**3**).

	$[(AuPPh_3)_2(cpa)]$ (**2**)	$[AgAu(PPh_3)_2(cpa)]$ (**3**)
(a) Au/Ag environment		
Au(1)/Ag(1)–P(1)	2.230(4)	2.315(3)
Au(2)–P(2)	2.264(4)	2.269(3)
Au(1)/Ag(1)–S(1)	2.356(4)	2.431(3)
Au(1)/Ag(1)–O(11)	2.537(12)	2.374(8)
Au(1)/Ag(1)–Au(2)	3.0338(10)	3.0463(10)
S(1)–Au(2)	2.333(3)	2.312(3)
P(1)–Au(1)/Ag(1)–S(1)	166.21(15)	159.81(10)
P(1)–Au(1)/Ag(1)–O(11)	117.2(3)	121.9(2)
S(1)–Au(1)/Ag(1)–O(11)	76.6(3)	78.3(2)
P(1)–Au(1)/Ag(1)–Au(2)	123.37(10)	121.9(2)
S(1)–Au(1)/Ag(1)–Au(2)	49.36(9)	48.35(6)
O(11)–Au(1)/Ag(1)–Au(2)	99.2(2)	100.9(2)
Au(2)–S(1)–Au(1)/Ag(1)	80.62(12)	79.87(8)
P(2)–Au(2)–S(1)	177.41(15)	176.78(10)
P(2)–Au(2)–Au(1)/Ag(1)	132.38(11)	131.38(7)
S(1)–Au(2)–Au(1)/Ag(1)	50.01(10)	51.78(7)
(b) cpa		
S(1)–C(2)	1.787(15)	1.820(10)
C(1)–O(12)	1.191(18)	1.231(13)
C(1)–O(11)	1.215(17)	1.238(12)
O(12)–C(1)–O(11)	125.7(19)	122.1(11)

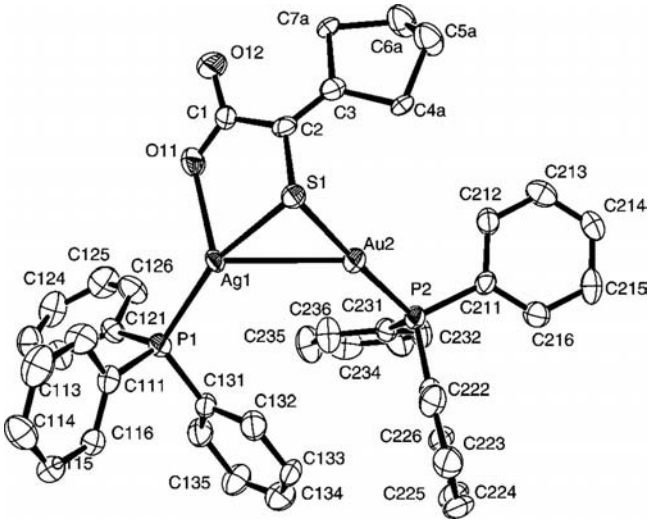

Figure 2. Structure of $[AgAu(PPh_3)_2(cpa)]$ (**3**) showing the numbering scheme. Ellipsoids are drawn at the 30% probability level.

The Ag(1)–Au(2) distance of 3.0463(10) Å, is only slightly longer than the Au(1)–Au(2) distance found in **2** of 3.0338(10) Å. To the best of our knowledge, isolated dinuclear units containing an S-supported Ag–Au interaction have not previously been reported in the literature. However, equivalent and shorter metal–metal distances were described for the dinuclear complexes $[AuAg\{CH_3im(CH_2py)\}_2](BF_4)_2$ [$CH_3im(CH_2py)$ = 1-methyl-3-(2-pyridinylmethyl)imidazole][20] and $[(dpim)_3AuAg](BF_4)_2$ [dpim = 2-(diphenylphosphanyl)-1-methylimidazole], respectively.[21] Shorter distances were also found in the trinuclear complex $[AuAg_2\{(pyCH_2)_2im\}_2(NCCH_3)_2](BF_4)_3$ [$(pyCH_2)_2im$ = 1,3-bis(2-pyridylmethyl)imidazole],[22] in the tetranuclear

cation $[\{(Ph_3P)Au(\mu\text{-mes})Ag(thz)\}_2]^{2+}$,[23] in the clusters $[Au_6Ag\{\mu\text{-}C_6H_2(CHMe_2)_3\}_6]^+$,[24] $[Au_3Ag(\mu_3\text{-}O)(PPh_2py)_3]^{2+}$,[25] $[Au_5Ag_8(\mu\text{-dppm})_4\{1,2,3\text{-}C_6(C_6H_5)_3\}(C{\equiv}CC_6H_5)_7]^{3+}$[26] and $(Bu_4N)_2[Au(3,5\text{-}C_6F_3Cl_2)_2Ag_4(CF_3COO)_5]$,[27,28] and in polymers such as $[\{Au(\mu\text{-mes})AsPh_3\}_2Ag](ClO_4)$,[29] $[AgAu(mtp)_2]$ (mtp = diphenylmethylenethiophosphinato),[30] $\{[AuAg(Meimpy)_2(L)](BF_4)_2\}_n$, $\{[AuAg(Meimpy)_2(NO_3)]NO_3\}_n$ (Meimpy = methylimidazolepyridine; L = CH_3CN, C_6H_5CN, $C_6H_5CH_2CN$),[31] $[Au_2Ag_2(C_6F_5)_4(OCMe_2)_2]_n$,[32] $[Au_2Ag_2(C_6F_5)_4(NCCH_3)_2]_n$,[33] or $Ag([Au(\mu\text{-}C^2,N^3\text{-bzim})]_3)_2{\cdot}BF_4{\cdot}CH_2Cl_2$,[34,35] $[AuAg_4(mes)(CF_3CO_2)_4(tht)]_n$, $[AuAg_4(mes)(CF_3CF_2CO_2)_4(tht)]_n$, $[AuAg_4(mes)(CF_3CF_2CO_2)_4(tht)_3]_n$, $\{[AuAg_4(mes)(CF_3CO_2)_4(tht)(H_2O)]{\cdot}H_2O{\cdot}CH_2Cl_2\}_n$,[17] $[AuAg_3(C_6F_5)(CF_3CO_2)_3(CH_2PPh_3)]_n$,[36] $[AgAu(C_6F_5)(CF_3CO_2)(tht)]_n$, $[Ag_2Au(C_6Cl_2F_3)(CF_3CO_2)_2(tht)]_n$, and $[AgAu(C_6Cl_5)(CF_3CO_2)(tht)]_n$.[18]

Single crystals obtained by slow concentration of an acetone solution of **4** were identified as $[(AgPPh_3)_2cpa]{\cdot}(CH_3)_2CO$. The tetranuclear $[(AgPPh_3)_2cpa]_2$ unit present in the crystal is shown in Figure 3 together with the numbering scheme, and selected distances and angles are listed in Table 2. As in **2** and **3** the S atom of the cpa ligand is bonded to two metal atoms, in this case two Ag atoms. One of these atoms, Ag(1), is also bonded to the O(1) atom of the carboxylato group [Ag(1)–O(1) 2.402(3) Å]. However, in contrast with complexes **2** and **3**, the O(1) and the O(2) atoms of the carboxylato group of this cpa ligand both bond in a slightly anisobidentate mode to Ag(2) [Ag(2)–O(1) 2.456(2) Å; Ag(2)–O(2) 2.562(3) Å]. These latter bonds create the tetranuclear $[(AgPPh_3)_2cpa]_2$ unit shown in Figure 3, in which an eight-membered $Ag_4O(1)_2S_2$ ring is present. In addition to the bonds that form this ring, each Ag atom is involved in an Ag–P bond, and the O(2) atom of the carboxylato group also participates in highly asymmetric Ag–O···Ag bridges [Ag(1)–$O(2)^{\#1}$ 2.712(3) Å]. This structural feature was previously detected in other (sulfanylcarboxylato)silver compounds[15] and, as in those compounds, in the case reported here there are (i) two types of Ag atoms with different environments [essentially tri-, Ag(1), and tetracoordinated, Ag(2),], (ii) Ag(1)–Ag(2) distances shorter than twice the van der Waals radius of silver (3.44 Å),[16] (iii) asymmetric Ag–S–Ag and Ag–O···Ag bridges, and (iv) longer Ag–P bonds for the PPh_3 ligand bonded to Ag(2) than for the equivalent ligand bonded to Ag(1).

The crystal of $[(AgPPh_3)_3(cpa)(NO_3)]{\cdot}(CH_3)_2CO$, [**5**·$(CH_3)_2CO$], contains hexanuclear $[(AgPPh_3)_3(cpa)(NO_3)]_2$ units, and these are shown in Figure 4 together with the numbering scheme, and selected bond lengths and angles are listed in Table 3. These units can be regarded as the result of two $Ag(PPh_3)NO_3$ fragments being added to the S atoms of the tetranuclear core previously discussed for **4**. Even though the essential features of this core remain unaltered after the addition of these two new fragments, there are slight structural changes that affect the distances and angles. The Ag(1)–S(1) and Ag(2)–$S(1)^{\#1}$ bonds in **4** [2.4402(12), 2.4822(14) Å] are only slightly longer in **5** [2.4819(12), 2.5139(11) Å], whereas the Ag(1)–S(1)–$Ag(2)^{\#1}$ angle of 79.38(3)° in **4** is slightly narrower in **5** [78.02(3)°]. The Ag(1)–O(1) distance is now shorter [2.379(3) Å vs. 2.402(3) Å in **4**], and the Ag(2)–O(1) and Ag(2)–O(2) distances [2.456(2), 2.562(3) Å, respectively, in **4**] are 2.557(3) and 2.452(3) Å in **5**, respectively. These distances signify a different anisobidentate behaviour for the carboxylato group, with the shortest Ag–O distance linking the O(2)

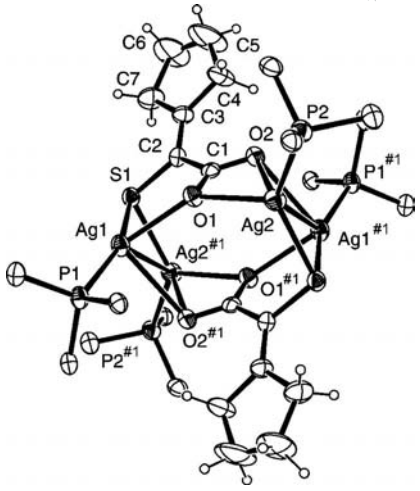

Figure 3. Structure of the dimeric unit present in $[(AgPPh_3)_2(cpa)]{\cdot}(CH_3)_2CO$ [**4**·$(CH_3)_2CO$], showing the numbering scheme. Ellipsoids are drawn at the 30% probability level. For the sake of clarity the phenyl groups of PPh_3 are not shown.

Table 2. Selected interatomic distances [Å] and angles [°] for complex $[(AgPPh_3)_2(cpa)]{\cdot}(CH_3)_2CO$ [**4**·$(CH_3)_2CO$].[a]

(a) Ag environment	
Ag(1)–P(1)	2.3604(13)
Ag(1)–O(1)	2.402(3)
Ag(1)–S(1)	2.4402(12)
Ag(1)–O(2)#1	2.712(3)
Ag(1)–Ag(2)#1	3.1439(9)
Ag(2)–P(2)	2.3982(13)
Ag(2)–O(1)	2.456(2)
Ag(2)–S(1)#1	2.4822(14)
Ag(2)–O(2)	2.562(3)
S(1)–Ag(2)#1	2.4822(14)
P(1)–Ag(1)–O(1)	118.56(7)
P(1)–Ag(1)–S(1)	159.50(4)
O(1)–Ag(1)–S(1)	80.36(7)
P(1)–Ag(1)–Ag(2)#1	130.83(3)
P(1)–Ag(1)–O(2)#1	89.75(6)
Ag(1)–O(1)–Ag(2)	142.02(12)
Ag(1)–S(1)–Ag(2)#1	79.38(3)
P(2)–Ag(2)–S(1)#1	132.49(4)
P(2)–Ag(2)–O(1)	121.01(7)
P(2)–Ag(2)–O(2)	106.40(7)
S(1)#1–Ag(2)–O(2)	103.38(6)
O(1)–Ag(2)–S(1)#1	106. 47(7)
O(1)–Ag(2)–O(2)	52.50(8)
(b) cpa	
S(1)–C(2)	1.770(4)
O(1)–C(1)	1.275(4)
C(1)–O(2)	1.258(4)
O(2)–C(1)–O(1)	122.5(4)

[a] #1: $-x, -y, -z + 1$.

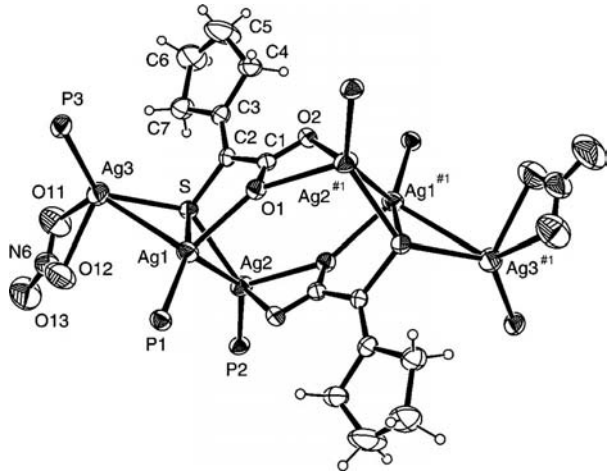

Figure 4. Structure of the hexanuclear units present in $[(AgPPh_3)_3(cpa)(NO_3)]\cdot(CH_3)_2CO$ [**5**·$(CH_3)_2CO$]. Ellipsoids are drawn at the 30% probability level. For the sake of clarity the phenyl groups of PPh_3 are not shown.

Table 3. Selected interatomic distances [Å] and angles [°] for complex $[(AgPPh_3)_3(cpa)(NO_3)]\cdot(CH_3)_2CO$ [**5**·$(CH_3)_2CO$].[a]

(a) Ag environment			
Ag(1)–P(1)	2.3606(12)	P(1)–Ag(1)–S(1)	153.90(5)
Ag(1)–S(1)	2.4819(12)	P(1)–Ag(1)–O(1)	125.56(8)
Ag(1)–O(1)	2.379(3)	S(1)–Ag(1)–O(1)	80.05(7)
Ag(1)–Ag(2)	3.1449(5)	P(1)–Ag(1)–Ag(2)	117.41(3)
Ag(1)–Ag(3)	3.1527(6)	O(1)–Ag(1)–Ag(2)	88.87(7)
Ag(2)–P(2)	2.4001(12)	S(1)–Ag(1)–Ag(2)	51.44(3)
Ag(2)–S(1)	2.5139(11)	P(1)–Ag(1)–Ag(3)	115.71(4)
Ag(2)–O(2)#1	2.452(3)	O(1)–Ag(1)–Ag(3)	107.07(7)
Ag(2)–O(1)#1	2.557(3)	S(1)–Ag(1)–Ag(3)	51.62(3)
Ag(3)–S(1)	2.5263(12)	Ag(2)–Ag(1)–Ag(3)	95.563(15)
Ag(3)–P(3)	2.3844(13)	P(2)–Ag(2)–S(1)	132.88(5)
Ag(3)–O(12)	2.427(5)	S(1)–Ag(2)–O(2)#1	106.43(7)
Ag(3)–O(11)	2.468(5)	S(1)–Ag(2)–O(1)#1	102.00(7)
		P(2)–Ag(2)–Ag(1)	142.79(3)
		O(2)#1–Ag(2)–Ag(1)	59.44(7)
		O(1)#1–Ag(2)–Ag(1)	86.88(6)
		P(2)–Ag(2)–O(1)#1	120.28(7)
		P(2)–Ag(2)–O(2)#1	115.24(7)
		O(2)#1–Ag(2)–O(1)#1	52.42(9)
		P(3)–Ag(3)–S(1)	129.55(5)
		P(3)–Ag(3)–O(12)	127.21(14)
		P(3)–Ag(3)–O(11)	120.88(12)
		O(12)–Ag(3)–O(11)	50.07(15)
		O(12)–Ag(3)–S(1)	100.74(13)
		O(11)–Ag(3)–S(1)	100.58(11)
		P(3)–Ag(3)–Ag(1)	109.35(4)
		O(12)–Ag(3)–Ag(1)	89.28(13)
		O(11)–Ag(3)–Ag(1)	127.86(12)
		Ag(1)–S(1)–Ag(2)	78.02(3)
		C(2)–S(1)–Ag(3)	109.59(14)
		Ag(1)–S(1)–Ag(3)	78.02(3)
		Ag(2)–S(1)–Ag(3)	135.44(5)
(b) cpa			
S–C(2)	1.785(4)	O(2)–C(1)–O(1)	122.4(4)
O(1)–C(1)	1.276(5)		
O(2)–C(1)	1.251(5)		
C(1)–C(2)	1.514(6)		
C(2)–C(3)	1.339(5)		

[a] #1: $-x + 2, -y + 2, -z$.

instead of the O(1) atom. As a result, the Ag(1)–O(1)–Ag(2) unit [for which the Ag–O–Ag angle changes from 142.02(12)° in **4** to 149.52(12)° in **5**] is now less symmetric. These structural changes do not significantly affect the distances between the two S-supported Ag atoms, which remain practically unchanged, but they do affect the distance between the two silver atoms that are bridged by the O(1) atom: 4.5935(11) Å in **4** vs. 4.7626(6) Å in **5**.

In compound **5** the two Ag atoms in the core, Ag(1) and Ag(2), retain the coordination mode found in **4**. Ag(1) is essentially SPO-tricoordinate [although with Ag(2) at 3.1449(5) Å and $O(2)^{\#1}$ at 2.839(3) Å] and Ag(2) is essentially SPO_2-tetracoordinate [with Ag(1) at 3.1449(5) Å]. The Ag(3) atom is also SPO_2-tetracoordinate, although the parameters for the coordination kernel are slightly different from those found for Ag(2). It is worth noting the shorter Ag–O bond lengths with the almost symmetrical bidentate nitrato ligand. Ag(3) is located 3.1527(6) Å from Ag(1) and, as discussed above, Ag(2) is at 3.1449(5) Å. The Ag(3)–Ag(1)–Ag(2) bond angle is 95.563(15)°, and the S atom, which acts as a triple bridge between these atoms, is located 0.94(1) Å from the Ag_3 plane.

It can be seen from Figure 5 that in the crystal structure, two of these hexanuclear units and two molecules of acetone interact through a C–H···O hydrogen bond [C(214)–H(214)···O(21)#1 0.93, 2.63, 3.553(9) Å, 170.5°; C(335)–H(335)···O(21) 0.93, 2.52, 3.380(10) Å, 154.8°] between the phenyl ring of the PPh_3 ligand and the O atom of $(CH_3)_2CO$.

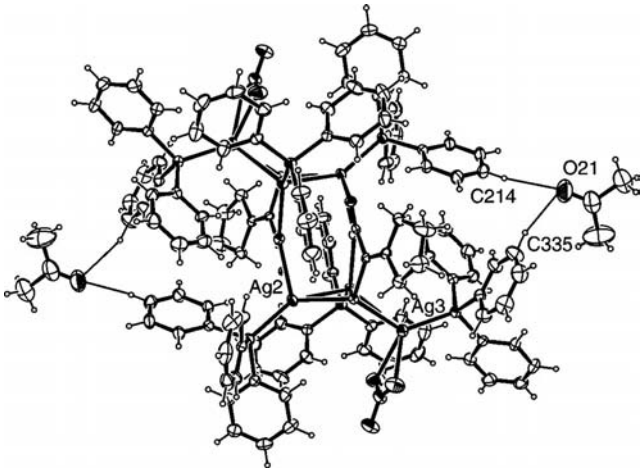

Figure 5. Hydrogen-bonding interactions between the $[(AgPPh_3)_3(cpa)(NO_3)]_2$ units and two molecules of $(CH_3)_2CO$ in $[(AgPPh_3)_3(cpa)(NO_3)]\cdot(CH_3)_2CO$ [**5**·$(CH_3)_2CO$].

Luminescence and Theoretical Studies

Complex **3** shows an emission at 374 nm (λ_{exc} = 273 nm) in a glassy EtOH/MeOH/CH_2Cl_2 (8:2:1) medium at 77 K but it does not show luminescence in the solid state or in solution, neither at room temperature nor at 77 K (see Figure 6). The emission band has a structured profile beginning at 358 nm (vibronic progression ca. 1100 cm^{-1}), and

this is consistent with the stretching frequencies of the ligands. This fact, together with the asymmetry of the emission band, suggests that an intraligand transition is responsible for the excited state that gives rise to the emission. More specifically, this process probably involves the phenyl rings or the carboxylato groups in the excited state.

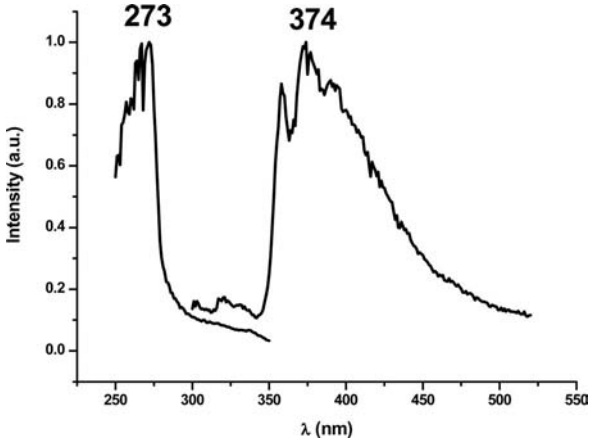

Figure 6. Excitation and emission spectra of complex **3** in a glassy EtOH/MeOH/CH_2Cl_2 (8:2:1) medium at 77 K.

Single-point DFT calculations were carried out on a model system of complex **3** built up from the X-ray diffraction coordinates. The electronic structure calculated by using the B3LYP functional shows that the HOMO orbital is mostly located on oxygen atoms of the cpa ligand, with some contribution from the thiolato moiety. Orbitals HOMO-1 to HOMO-5 are also mostly centred on the cpa ligand and on the gold(I) and silver(I) centres. The results of a population analysis, which show the contribution of each part of the molecule to the highest occupied molecular orbitals, are given in Table 4, and the shapes of the frontier orbitals are shown in Figure 7. The lowest unoccupied molecular orbitals LUMO to LUMO+6 are located on the phenyl rings of the triphenylphosphane ligands bonded to Au^I and Ag^I, with the first metal-based empty molecular orbital being LUMO+11. Taking into account these theoretical results and the photophysical measurements, it seems plausible that intraligand electronic transitions are the origin of the luminescent behaviour of complex **3**. A possible ^{3}LMCT origin[11] from the thiolato moiety of the cpa ligand to the gold(I) centre can be ruled out since the orbitals involved in this transition are markedly different in energy, and a preference for an IL intraligand transition involving the cpa ligand and the phenyl rings of the triphenylphosphane ligands is more likely in view of the shapes of the frontier orbitals.

Table 4. Population analysis for the model system representing complex **3**. Contribution from each part of the molecule to the occupied orbitals.

Molecular orbital	% Au	%Ag	% cpa ligand[a]
HOMO	1.1	4.2	85.6
HOMO-1	1.0	1.8	88.8
HOMO-2	1.3	6.4	83.1
HOMO-3	3.9	4.2	82.4
HOMO-4	14.0	27.2	48.1

[a] The contribution from PPh_3 ligands to these molecular orbitals is not relevant.

NMR Spectroscopic Studies

^{1}H and ^{13}C NMR spectroscopy was used to investigate the coordination of the cpa and PPh_3 ligands. The ^{1}H NMR spectrum of **1** shows a very broad signal at δ = 12.30 ppm, and this can be assigned to the CO_2H proton. This signal is not observed in the spectra of **2**, **3** and **4** due to the deprotonation of this group upon formation of the three complexes. A multiplet can be observed at $\delta \approx 7.5$ ppm in the spectra of the four complexes due to the PPh_3 ligand. In the ^{13}C NMR spectra of **2**, **3** and **4** the position of the C(1) signal, $\delta \approx 170$ ppm, is typical[37] of a monodentate carboxylato group, suggesting that the interaction of the metal atoms with the O atom persists in solution. The slight deshielding of C(2) with respect to that in the free ligand, together with the shielding experienced by C(3), indicates that the S atom also remains coordinated to the metal atom in solution.[38] The C-*ipso* signal of the PPh_3 ligand is shifted to higher field in the complexes, and the $^1J_{^{13}C,^{31}P}$ value is also higher, providing evidence that this ligand also remains coordinated in solution.[39]

^{31}P NMR spectroscopy was used to gain additional information about the coordination number of the Ag atom in **3** and **4**. The ^{31}P NMR chemical shift has previously been used as a diagnostic tool for the Ag coordination

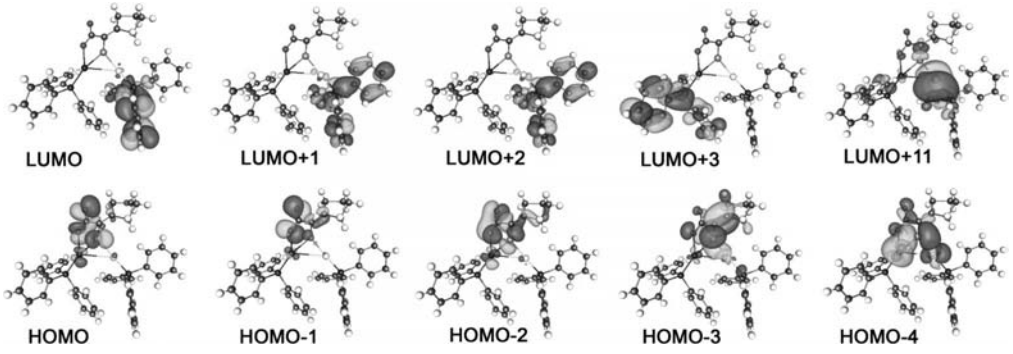

Figure 7. Frontier occupied and empty orbitals for the model system of complex **3**.

number in PPh_3 complexes by relating the shielding with the increase in the metal coordination number.[40,41] However, the magnitude of $^1J_{^{31}P,^{109,107}Ag}$ has proven to be more appropriate for structural studies due to the fact that the coupling constants decrease substantially as the coordination number increases.[42,43]

The high kinetic lability of monodentate phosphanes generally leads to rapid ligand exchange on the NMR timescale[43] and, as a result, most of the spectra obtained at 25 °C (see Figure S1, Supporting Information) contain broad peaks. Low-temperature $^{31}P\{^1H\}$ NMR experiments were therefore used, and the appropriate solvent was selected for each compound (see Experimental Section and Table S1, Supporting Information). The appropriate temperature to obtain the characteristic ^{31}P–$^{109,107}Ag$ doublet of doublets for each P environment, which results from the coupling of the P atom to each of the spin $I = 1/2$ silver isotopes (^{107}Ag, 51.8% natural abundance; ^{109}Ag, 48.2% natural abundance), was determined. The data for these experiments are given in Table S1, Supporting Information.

The spectrum of **3** at room temperature in CD_2Cl_2 (Figure S1, Supporting Information) consists of two very broad peaks located at $\delta = 37.2$ ppm ($w_{1/2} = 1230$ Hz) and 16.1 ppm ($w_{1/2} = 1560$ Hz). On the basis of the data for **2** and **4**, as well as previous data,[12,15] these signals were attributed to the Au and Ag atoms bonded to PPh_3, respectively. At a temperature of 213 K, the low-field peak appeared as a singlet at $\delta = 36.2$ ppm, but the high-field signal was split into the characteristic doublet of doublets due to the coupling of the P nucleus with the two Ag natural isotopes, centred at $\delta = 14.3$ ppm (Figure 8). This observation confirms that this signal is due to the PPh_3 ligand bonded to the Ag atom and also that the Ag–P interaction is retained in solution. The $^1J_{^{31}P,^{109,107}Ag}$ values of 672 and 582 Hz are comparable to those reported in the literature (ref.[44] and references cited therein) for triphenylphosphane complexes containing silver(I) with a coordination number ≤ 3.[42,44,45]

The behaviour of compound **4** in solution is more complicated. The room-temperature $^{31}P\{^1H\}$ NMR spectra in the solvents used (see Table S1, Supporting Information) each contain a single signal for the two PPh_3 ligands, which are more shielded than those in compound **3**. The spectrum in $[D_7]$DMF solution at 209 K reveals two broad doublets centred at $\delta = 9.66$ and 3.93 ppm with $^1J_{^{31}P,Ag}$ values of 333 and 291 Hz, respectively. The chemical shifts are indicative of two different environments for the ligand, and the coupling constants are compatible with a tetrahedral arrangement around the metal centre.[42,44,45] The spectrum recorded at 193 K ($[D_7]DMF/CD_2Cl_2$, 1:1) consists of two well-resolved doublets of doublets at $\delta = 7.75$ ppm [$^1J_{^{31}P,^{109,107}Ag} = 258$ and 224 Hz] and 4.72 ppm [$^1J_{^{31}P,^{109,107}Ag} = 315$ and 272 Hz]. The ^1J values are consistent with a tetrahedral environment for the silver atoms, although the differences in the ^1J values could be associated with a slightly different environment for the two silver atoms.[42,44–46] In CD_2Cl_2 solution at 213 K only one doublet of doublets, centred at $\delta = 5.18$ ppm [$^1J_{^{31}P,^{109,107}Ag} = 257$ and 223 Hz], was detected, and the δ and ^1J values indicate the existence of a unique environment for the silver(I) atom with a tetrahedral geometry.

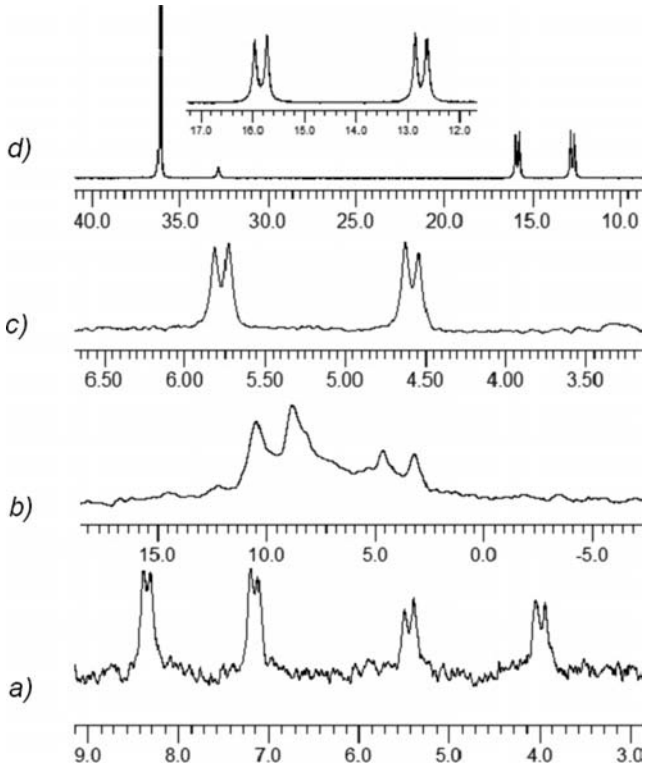

Figure 8. $^{31}P\{^1H\}$ NMR spectra (δ scale in ppm; referenced to external 85% H_3PO_4) of $[(AgPPh_3)_2(cpa)]$ (**4**): (a) measured in $[D_7]$-DMF/CD_2Cl_2 at 193 K; (b) measured in $[D_7]$DMF at 209 K; (c) measured in CD_2Cl_2 at 213 K and (d) of $[AgAu(PPh_3)_2(cpa)]$ (**3**) measured in $CDCl_3$ at 213 K.

Low-temperature measurements also enabled us to determine the coalescence temperature (T_c) in each experiment, and these data were subsequently used in thermodynamic studies. Bearing in mind previously published equations,[47,48] we were able to calculate the activation energy, $\Delta G(T_c)^{\ddagger}$, and the rate constants, k_c, for the ligand exchange discussed above. The data are presented in Table S1, Supporting Information. The activation-energy values, which are between 41.5 and 45.5 kJ mol^{-1}, are comparable with values reported previously for (diphenylphosphane)silver(I) complexes.[49] On the other hand, the k_c values (see Table S1, Supporting Information) indicate that the PPh_3 ligand lability in $[AgAu(PPh_3)_2cpa]$ is higher than that in $[(AgPPh_3)_2cpa]$ in the same solvent.

Cytotoxicity in Human Cervix Carcinoma and Human Ovarian Carcinoma Cells

The difference between compounds **2** and **3** is the replacement of an Au atom by an Ag atom. The influence of this substitution on cytotoxicity was assessed by comparing the activity of each compound against the human Hela-229 cervix carcinoma cell line and the A2780 ovarian carcinoma cell line along with its cisplatin-resistant mutant A2780cis.

For comparative purposes, the cytotoxicity of cisplatin was also evaluated under the same experimental conditions.

We previously studied the activity of the free H_2cpa ligand, which has only a small effect on cell growth. At 50 μM the cell-growth inhibition percentages are 1 (HeLa), 6 (A2780) and 3 (A2780cis) and, as a result, the corresponding IC_{50} values were not calculated. The values obtained against these three lines are shown in Table 5 for compounds **2** and **3**. The values are in the low μM range, and both compounds are similar, with **2** being only slightly better than **3**. In both cases the activity follows the general trend A2780 > A2780cis > HeLa, which was previously found for (thiolato)gold complexes[13,50] and is in contrast with the results obtained for cisplatin, which is less active against the A2780cis line. These data show that compounds **2** and **3** are able to avoid the multifactorial resistance mechanism that in the latter cell line affects cisplatin and other platinum-based anticancer agents, as demonstrated by the values (< 2) of the resistance factor [$RF = IC_{50}$(A2780cis)/IC_{50}(A2780)] listed in Table 5.[51]

Table 5. In vitro cytotoxicity (IC_{50} [μM]) against HeLa, A2780 and A2780cis cell lines.

Compound	HeLa[a]	A2780[b]	A2780cis[b]	RF[c]
[Au(PPh_3)(Hcpa)] (**1**)	4.0 (0.5)	0.77 (0.1)	3.10 (0.6)	4.05
[($AuPPh_3$)$_2$cpa] (**2**)	2.2 (0.4)	1.09 (0.07)	1.51 (0.08)	1.4
[AgAu(PPh_3)$_2$cpa] (**3**)	3.1 (0.03)	1.65 (0.02)	1.99 (0.04)	1.2
Cisplatin	0.53 (0.06)	0.44 (0.06)	3.6 (0.5)	8.2

[a] 48 h incubation. [b] 96 h incubation. [c] The resistance factor: $RF = IC_{50}$(A2780cis)/IC_{50}(A2780).

Conclusions

The reaction of [Au(PPh_3)(Hcpa)] with Ag(PPh_3)NO_3 and NaOH gave the complex [AgAu(PPh_3)$_2$cpa], which is dinuclear and has S- and P-bonded Au and Ag atoms. The latter metal centre is also O-bonded. Theoretical studies suggest that intraligand electronic transitions give rise to the luminescence behaviour of this compound, and in vitro studies showed significant cytotoxicity against HeLa, A2780 and A2780cis cell lines. This cytotoxicity was equivalent to that found for [($AuPPh_3$)$_2$cpa], which was prepared for comparative purposes. This gold(I) compound is also dinuclear, but the equivalent silver(I) compound [($AgPPh_3$)$_2$-cpa], also prepared for comparative purposes, is tetranuclear and, as revealed by the structure of the hexanuclear [($AgPPh_3$)$_3$(cpa)(NO_3)] unit, this could incorporate additional metal atoms. ^{1}H and ^{13}C NMR spectroscopic data suggest that the S, O and P atoms of the cpa and the phosphane ligands remain coordinated in solution. The rapid ligand exchange (on the NMR time scale) of the coordinated phosphanes was identified by room-temperature ^{31}P NMR spectroscopy. Thermodynamic parameters related to the kinetic lability of the phosphane ligands were calculated on the basis of low-temperature experiments.

Experimental Section

Materials and Methods: Cyclopentanone (99%), rhodanine and (triphenylphosphane)gold(I) chloride (all from Aldrich) were used as supplied. Ag(PPh_3)(NO_3) was synthesised by treating $AgNO_3$ with PPh_3 in CH_3CN/methanol. 2-Cyclopentylidene-2-sulfanylacetic acid, H_2cpa, was prepared by condensation of cyclopentanone with rhodanine, subsequent alkaline hydrolysis of the resultant 5-substituted rhodanine[52] and acidification with aqueous HCl.[53] Elemental analyses were performed with a Fisons 1108 microanalyser. Melting points were determined with a Büchi apparatus and are uncorrected. IR spectra (KBr pellets or Nujol mulls) were recorded with a Bruker IFS66V FTIR spectrophotometer and are reported in the synthesis section by using the following abbreviations: vs. = very strong, s = strong, m = medium, w = weak, sh = shoulder, br. = broad. Mass spectra were recorded in methanol with a Hewlett Packard 1100 LC/MSD spectrometer by using positive or negative electrospray ionisation. ^{1}H and ^{13}C NMR spectra were recorded in [D_6]DMSO, $CDCl_3$ or [D_7]DMF at room temperature with a Bruker AMX 300 spectrometer operating at 300.14 and 75.40 MHz, respectively, by using 5 mm o.d. tubes; chemical shifts are reported relative to TMS by using the solvent signals [δ(^{1}H) = 2.50 ppm, δ(^{13}C) = 39.5 ppm for [D_6]DMSO and δ(^{1}H) = 8.01 ppm, δ(^{13}C) = 162.7 ppm in [D_7]DMF] as references. ^{31}P NMR spectra were recorded in [D_6]DMSO, $CDCl_3$, CD_2Cl_2 or [D_7]DMF at 202.46 MHz with a Bruker AMX 500 spectrometer by using 5 mm o.d. tubes and are reported relative to external H_3PO_4 (85%). Signals are described as follows: chemical shift; multiplicity (s = singlet, d = doublet, dd = doublet of doublets, m = multiplet, br. s = broad singlet, v. br. s = very broad singlet); relative integral (for ^{1}H); and coupling constants J in Hz. All the physical measurements were carried out by the RIAIDT services of the University of Santiago de Compostela (USC).

Synthesis: The complex [Au(PPh_3)(Hcpa)] was prepared by adding Au(PPh_3)Cl to a solution of H_2cpa and KOH in a 1:1:1 molar ratio in ethanol/water (4:1, v/v). The mixture was stirred for 1 h, and the solvent was evaporated under vacuum. The resultant solid was washed with water and dried under vacuum. The complex [($AuPPh_3$)$_2$cpa] was prepared by adding Au(PPh_3)Cl in a 2:1 molar ratio to a solution of H_2cpa and NaOH in methanol/water. The mixture was stirred for 1 h, and the solvent was evaporated. The resultant solid was washed with water and dried under vacuum. The complex [AgAu(PPh_3)$_2$cpa] was synthesised by treating [Au(PPh_3)(Hcpa)] with Ag(PPh_3)NO_3 in a 1:1 molar ratio in methanol. The mixture was stirred at room temperature in the dark for 24 h, and the solid was filtered off, washed with water and dried under vacuum.

[Au(PPh_3)(Hcpa)] (1): H_2cpa (0.042 g, 3.0×10^{-4} mol), $AuPPh_3Cl$ (0.15 g, 3.0×10^{-4} mol), ethanol (12 cm^3), KOH (0.016 g, 3.0×10^{-4} mol), H_2O (3 cm^3). Pale-brown solid. Yield: 0.12 g, 78%. M.p. 65 °C. $C_{25}H_{24}AuO_2PS$ (616.46): calcd. C 48.71, H 3.92, S 5.20; found C 48.53, H 3.82, S 4.94. IR: $\tilde{\nu}$ = 1662 (s, ν, C=O) 1436 (s, δ, OH) 1272 (m, ν, C–O) 1479 (m), 1436 (s) (ν, PPh_3) cm^{-1}. Main metallated ESI-MS (+) peaks: *m*/*z* (%) = 1409 (29) [($AuPPh_3$)$_3$S]$^+$, 1075 (91) [($AuPPh_3$)$_2$cpa]$^+$, 721 (28) [Au(PPh_3)$_2$]$^+$, 617 (3) [(M)]$^+$, 459 (4) [($AuPPh_3$)]$^+$. NMR ([D_6]DMSO): ^{1}H: δ = 12.30 [s, 1 H, C(1)OH], 3.32 [m, 2 H, C(4)H_2], 1.61 [m, 2 H, C(5)H_2], 1.61 [m, 2 H, C(6)H_2], 3.32 [m, 2 H, C(7)H_2], 7.46–7.61 [m, 15 H, H(PPh_3)] ppm. ^{13}C: δ = 171.1 C(1), 121.2 C(2), 151.8 C(3), 35.5 C(4), 27.3 C(5), 25.4 C(6), 34.0 C(7), 129.1 [d, C_i(Ph_3), $^1J_{^{13}C,^{31}P}$ = 56.5 Hz], 133.7 [d, C_o(Ph_3), $^2J_{13C,31P}$ = 13.7 Hz], 129.5 [d, C_m(Ph_3), $^3J_{^{13}C,^{31}P}$ = 12.2 Hz], 132.0 [s, C_p(Ph_3)] ppm. ($CDCl_3$): ^{31}P{^{1}H}: δ = 35.5 (s) ppm.

[(AuPPh$_3$)$_2$cpa] (2): H_2cpa (0.024 g, 1.5×10^{-4} mol), Au(PPh$_3$)Cl (0.15 g, 3.0×10^{-4} mol), methanol (12 cm^3), NaOH (0.012 g, 3.0×10^{-4} mol), H_2O (3 cm^3). White solid. Yield: 0.12 g, 73%. M.p. 156 °C. $C_{43}H_{38}Au_2O_2P_2S$ (1074.71): calcd. C 48.06, H 3.56, S 2.98; found C 47.94, H 3.25, S 3.10. IR: $\tilde{\nu}$ = 1579 (vs, ν_a, CO_2) 1481 (m), 1436 (s) (ν, PPh$_3$) cm^{-1}. Main metallated ESI-MS (+) peaks. *m/z* (%) = 1409 (97) [(AuPPh$_3$)$_3$S]$^+$; 1075 (8) [M]$^+$; 721 (12) [Au(PPh$_3$)$_2$]$^+$; 459 (2) [(AuPPh$_3$)]$^+$. NMR ([D$_6$]DMSO): ^{1}H: δ = 3.00 [m, 2 H, C(4)H$_2$], 1.68 [m, 2 H, C(5)H$_2$], 1.68 [m, 2 H, C(6)H$_2$], 2.80 [m, 2 H, C(7)H$_2$], 7.35–7.59 [m, 30 H, H(PPh$_3$)] ppm. ^{31}P{^{1}H}: δ = 36.8 (s) ppm. ([D$_7$]DMF): ^{1}H: δ = 2.61 [v. br. s, C(4)H$_2$], 1.57 [br. s, C(5)H$_2$], 1.57 [br. s, C(6) H$_2$], 2.61 [v. br. s, C(7) H$_2$], 7.55–7.65 [m, H(PPh$_3$)] ppm. ^{13}C: δ = 121.7 C(2), 153.4 C(3), 36.3 C(4), 26.0 C(5), 25.9 C(6), 34.6 C(7), 129.8 [d, C_i(Ph$_3$), $^1J_{^{13}C,^{31}P}$ = 59.2 Hz], 134.7 [d, C_o(Ph$_3$), $^2J_{^{13}C,^{31}P}$ = 13.8 Hz], 130.3 [d, C_m(Ph$_3$), $^3J_{^{13}C,^{31}P}$ = 11.6 Hz], 132.9 [s, C_p(Ph$_3$)] ppm. (CDCl$_3$): ^{31}P{^{1}H}: δ = 31.9 (s) (room temp.), 31.1 (s) (low temp., 213 K) ppm. Single crystals of **2** were grown by slow concentration of the mother liquor.

[AgAu(PPh$_3$)$_2$cpa] (3): [Au(PPh$_3$)(Hcpa)] (0.10 g, 0.16×10^{-4} mol), Ag(PPh$_3$)NO$_3$ (0.07 g, 0.16×10^{-4} mol), NaOH (6.49 10^{-3} g, 0.16×10^{-4} mol), methanol (15 cm^3). White solid. Yield: 0.11 g, 68%. M.p. 178 °C. $C_{43}H_{38}AgAuO_2P_2S$ (985.61): calcd. C 52.40, H 3.89, S 3.25; found C 51.94, H 3.90, S 3.40%. IR: $\tilde{\nu}$ = 1577 (vs, ν_{as}, COO) 1480 (s), 1436 (vs), (ν, PPh$_3$) cm^{-1}. Main metallated ESI-MS (+) peaks: *m/z* (%) = 1409 (0.5) [(AuPPh$_3$)$_3$S]$^+$, 1075 (6) [(AuPPh$_3$)$_2$-cpa]$^+$, 986 (5) [(M)]$^+$, 721 (100) [Au(PPh$_3$)$_2$]$^+$, 631 (0.8) [(PPh$_3$)$_2$-Ag]$^+$, 459 (0.3), [(PPh$_3$)Au]$^+$, 369 (1) [(PPh$_3$)Ag]$^+$. NMR ([D$_6$]-DMSO): ^{1}H: δ = 2.74 [m, 2 H, C(4)H$_2$], 1.55 [m, 2 H, C(5)H$_2$], 1.55 [m, 2 H, C(6) H$_2$], 2.60 [m, 2 H, C(7) H$_2$], 7.27–7.74 [m, 30 H, H(PPh$_3$)] ppm. ^{13}C: δ = 171.1 C(1), 122.7 C(2), 152.2 C(3), 36.8 C(4), 27.4 C(5), 25.5 C(6), 34.7 C(7), 130.0 [d, C_i(Ph$_3$), $^1J_{^{13}C,^{31}P}$ = 43.9 Hz], 133.5 [d, C_o(Ph$_3$), $^2J_{^{13}C,^{31}P}$ = 15.5 Hz], 129.1 [d, C_m(Ph$_3$), $^3J_{^{13}C,^{31}P}$ = 10.3 Hz], 131.2 [s, C_p(Ph$_3$)] ppm. ^{31}P{^{1}H}: δ = 16.0 (s), 39.9 (s) ppm. Single crystals of **3** were grown by slow concentration of an acetone solution.

[(AgPPh$_3$)$_2$cpa] (4): H_2cpa (0.018 g, 1.16×10^{-4} mol), Ag(PPh$_3$)NO$_3$ (0.10 g, 1.16×10^{-4} mol), NaOAc (0.014 g, 1.71×10^{-4} mol), $CHCl_3$ (10 cm^3), H_2O (22 cm^3). White solid. Yield: 0.079 g, 65%. M.p. 165 °C. $C_{43}H_{38}Ag_2O_2P_2S$ (896.52): calcd. C 57.61, H 4.27, S 3.58; found C 57.91, H 4.60, S 3.45. IR: $\tilde{\nu}$ = 1534 (vs, ν_{as}, COO) 1479 (s), 1435 (vs) (ν, PPh$_3$) cm^{-1}. Main metallated ESI-MS (+) peaks: *m/z* (%) = 897 (2) [(M)]$^+$, 631 (19) [(PPh$_3$)$_2$Ag]$^+$, 369 (1) [(AgPPh$_3$)]$^+$. NMR ([D$_6$]DMSO): ^{1}H: δ = 2.59 [m, 2 H, C(4)H$_2$], 1.35 [m, 2 H, C(5)H$_2$], 1.29 [m, 2 H, C(6)H$_2$], 2.48 [m, 2 H, C(7) H$_2$] 7.20–7.55 [m, 30 H, H(PPh$_3$)] ppm. ^{13}C: δ = 170.8 C(1), 122.3 C(2), 155.9 C(3), 38.3 C(4), 27.6 C(5), 25.4 C(6), 35.3 C(7), 132.7 [d, C_o(Ph$_3$), $^2J_{^{13}C,^{31}P}$ = 12.5 Hz], 129.3 [d, C_m(Ph$_3$), $^3J_{^{13}C,^{31}P}$ = 9.8 Hz], 130.1 [s, C_p(Ph$_3$)] ppm. ^{31}P{^{1}H}: δ = 9.7 (s) ppm. Single crystals of [(AgPPh$_3$)$_2$cpa]·(CH$_3$)$_2$CO, (**4**)·(CH$_3$)$_2$CO, were grown by slow concentration of an acetone solution of **4**. In an attempt to purify an impure sample of **4** by using acetone as solvent a minimal amount of crystals was obtained. These crystals proved to be [(AgPPh$_3$)$_3$(cpa)(NO$_3$)]·(CH$_3$)$_2$CO, (**5**)·(CH$_3$)$_2$CO.

Crystallography: Single crystals of [(AuPPh$_3$)$_2$cpa] (**2**), [AgAu(PPh$_3$)$_2$cpa] (**3**) [(AgPPh$_3$)$_2$cpa]·(CH$_3$)$_2$CO [**4**·(CH$_3$)$_2$CO] and [(AgPPh$_3$)$_3$(cpa)(NO$_3$)]·(CH$_3$)$_2$CO [**5**·(CH$_3$)$_2$CO] were mounted on glass fibres for data collection with a Bruker Smart CCD automatic diffractometer at 293 K using Mo-K_α radiation (λ = 0.71073 Å). The crystal data, experimental details and refinement results are summarised in Table 6. Corrections for Lorentz effects, polarisation[54] and absorption[55a] were made. The structures were solved by direct methods and refined by full-matrix least squares on F^2 by using SHELXL.[55b] Data for the compounds presented a low numbers of reflections at higher angles than expected although the data are ca. 95% at 2θ = 50°. The refined goodness-of-fit values for compounds **2**, **4** and **5** are close to the lower limit of the range expected (0.8–2.0). However, the model seems correct (in every case), and optimisation of every weighting scheme was performed in the last stage of the refinement. The two effects are not significant and can be attributed to the low quality of the crystals. In the

Table 6. Crystal data for [(AuPPh$_3$)$_2$(cpa)] (**2**), [AgAu(PPh$_3$)$_2$(cpa)] (**3**), [(AgPPh$_3$)$_2$(cpa)]·(CH$_3$)$_2$CO [**4**·(CH$_3$)$_2$CO] and [(AgPPh$_3$)$_3$-(cpa)(NO$_3$)]·(CH$_3$)$_2$CO [**5**·(CH$_3$)$_2$CO].

	2	**3**	**4**·(CH$_3$)$_2$CO	**5**·(CH$_3$)$_2$CO
Empirical formula	$C_{43}H_{38}Au_2O_2P_2S$	$C_{43}H_{38}AgAuO_2P_2S$	$C_{46}H_{44}Ag_2O_3P_2S$	$C_{64}H_{59}Ag_3NO_6P_3S$
M	1074.67	985.57	954.55	1386.70
T [K]	293(2)	293(2)	173(2)	293(2)
Crystal system	triclinic	triclinic	monoclinic	triclinic
Space group	$P\bar{1}$	$P\bar{1}$	$P2_1/n$	$P\bar{1}$
a [Å]	12.4085(18)	12.498(3)	15.549(5)	14.7303(9)
b [Å]	12.5619(17)	12.515(3)	16.072(5)	14.7933(9)
c [Å]	13.9127(19)	13.894(3)	18.371(5)	17.1408(10)
a [°]	76.745(3)	77.919(4)		114.2530(10)
β [°]	74.162(3)	73.641(4)	110.390(5)	98.1500(10)
γ [°]	76.554(3)	77.316(4)		110.6810(10)
V [Å^3]	1997.0(5)	2009.0(7)	4303(2)	3000.5(3)
Z	2	2	4	2
D_c [Mg m^{-3}]	1.787	1.629	1.473	1.535
μ [mm^{-1}]	7.505	4.300	1.071	1.135
Crystal size [mm]	0.17 × 0.09 × 0.06	0.27 × 0.24 × 0.14	0.36 × 0.19 × 0.09	0.15 × 0.27 × 0.28
θ range for data collection [°]	2.24–28.12	1.55–28.10	1.89–28.04	1.57–28.03
Index ranges	$-16 \le h \le 15$	$-15 \le h \le 16$	$-20 \le h \le 15$	$-19 \le h \le 15$
	$-13 \le k \le 16$	$-6 \le k \le 16$	$-20 \le k \le 21$	$-17 \le k \le 19$
	$-17 \le l \le 18$	$-18 \le l \le 18$	$-18 \le l \le 23$	$-21 \le l \le 22$
Reflections collected	10892	13405	23794	17178
Unique reflections (*R*)	7696 (R_{int} = 0.0695)	9289 (R_{int} = 0.0721)	9611 (R_{int} = 0.0654)	12020 (R_{int} = 0.0298)
Final R_1, wR_2 [$I > 2\sigma(I)$]	0.0539, 0.0839	0.0608, 0.1477	0.0416, 0.0464	0.0402, 0.0678
Final *R* indices (all data)	0.2003, 0.1055	0.1259, 0.1688	0.1510, 0.0582	0.1077, 0.079399

case of [$(AuPPh_3)_2$cpa] (**2**), the refinement includes a temperature factor that is common to the C(5) and C(6) atoms. The presence of solvent in the net was studied with the SQUEEZE routine of PLATON[56] due to the presence of accessible voids. However, the low electron count/cell (10) calculated and the worse discrepancy factors obtained in the refinement precluded the inclusion of SQUEEZE corrections in the model. The cyclopentylidene fragment is disordered in the structure of **3**. This disorder was modelled by including two alternative positions for the carbon atoms, except C(3), with occupancy factors of 48 and 52%. CCDC-779238 (**2**), -779239 (**3**), -779240 [**4**·$(CH_3)_2CO$], and -779241 [**5**·$(CH_3)_2CO$] contain the supplementary crystallographic data for this paper. These data can be obtained free of charge from The Cambridge Crystallographic Data Centre via www.ccdc.cam.ac.uk/data_request/cif.

Luminescence and Theoretical Studies

Luminescence Measurements: Excitation and emission spectra at 77 K were recorded with a Jobin–Yvon Horiba Fluorolog 3–22 Tau-3 spectrofluorimeter.

Computational Details for DFT and TD-DFT Calculations: The model system used in the theoretical studies of complex [$AgAu(PPh_3)_2$cpa] (**3**) was taken from the X-ray diffraction data for complex **3**. Keeping all distances, angles and dihedral angles frozen, single-point DFT calculations were performed on this model system. In the ground-state calculations, the B3LYP functional[57] as implemented in TURBOMOLE[58] was used. In all calculations, the Karlsruhe split-valence quality basis sets[59] augmented with polarisation functions[60] were used (SVP). The Stuttgart effective core potential in TURBOMOLE was used for Au and Ag.[61]

In vitro Antitumor Activity

Cell Line and Growth Conditions: The human cervix carcinoma cell line HeLa-229 used in this study was kindly provided by Dr. Guadalupe Mengod (CSIC-IDIBAPS of Barcelona, Spain). Human ovarian cancer cell line A2780 and its cisplatin-resistant mutant A2780cis were obtained from the European Collection of Cell Cultures through Sigma–Aldrich. The cells were grown in Dulbecco's Modified Eagle's Medium (DMEM, HeLa-229) or RPMI 1640 medium (A2780, A2780cis) supplemented with 10% foetal calf serum (FCS) and 2 mM L-glutamine. Cells were maintained in continuous growth in a humidified atmosphere of 5% CO_2 at 37 °C and were harvested by using trypsin-ethylenediaminetetraacetic acid. All media and supplements were purchased from Sigma-RBI, Spain.

In vitro Chemosensitivity Assay: The cells were seeded into 96-well plates (Beckton-Dickinson, Spain) at a volume of 100 μL with a number of 4000 cells per well, and the samples were incubated for 4–6 h (HeLa-229) or 24 h (A2780, A2780cis) prior to dosage. Solutions of the complexes in ethanol were added to the cells by using the same concentration of ethanol per well (1%). After the appropriate incubation time, i.e. 48 h for HeLa-229 and 96 h for A2780 and A2780cis, the cells were fixed by adding 10 μL of 11% glutaraldehyde per well for 15 min. The fixative was then removed, and the wells were washed four times with distilled water. Cell biomass was determined by a crystal violet staining technique[62] and the optical density was measured at 595 nm with a Tecan Ultra Evolution microplate reader. Each complex was tested by using six or seven consecutive dilutions ranging from 50 μM to 0.025 μM. The compound concentration able to inhibit cell growth by 50% with respect to controls, IC_{50}, was then determined from semi-logarithmic dose-response sigmoid curves by using GraphPad Prism Ver. 2.01 software (GraphPad Software Inc.).[63] The cytotoxicity of the free ligand, $Au(PPh_3)Cl$, and that of cisplatin (dissolved in water) were evaluated for comparative purposes under the same experimental conditions. All compounds were tested in three independent experiments with quadruplicate points. The studies were performed in the unit for the evaluation of pharmacological activities of chemical compounds of the RIAIDT services of the USC.

Supporting Information (see footnote on the first page of this article): Table S1 and Figure S1 including $^{31}P\{^1H\}$ NMR spectroscopic data.

Acknowledgments

We thank the Spanish Ministry of Science and Technology (Projects BQU2002-04524-C02-01 and BQU2002-04524-C02-02) and the Spanish Ministry of Science and Innovation (Projects CTQ2010-20500-C02-01 and CTQ2010-20500-C02-02) for financial support.

[1] C. F Shaw, in *Gold: Progress in Chemistry, Biochemistry and Technology* (Ed.: H. Schmidbaur), J. Wiley & Sons, Chichester, UK, **1999**.
[2] H. E. Abdou, A. A. Mohamed, J. P. Fackler Jr., A. Burini, R. Galassi, J. M. López-de-Luzuriaga, M. E. Olmos, *Coord. Chem. Rev.* **2009**, *253*, 1661.
[3] I. Ott, *Coord. Chem. Rev.* **2009**, *253*, 1670.
[4] F. Magherini, A. Modesti, L. Bini, M. Puglia, I. Landini, S. Nobili, E. Mini, M. A. Cinellu, C. Gabbiani, L. Messori, *J. Biol. Inorg. Chem.* **2010**, *15*, 573.
[5] P. J. Barnard, L. E. Wedlock, M. V. Baker, S. J. Berners-Price, D. A. Joyce, B. W. Skelton, J. H. Steer, *Angew. Chem. Int. Ed.* **2006**, *45*, 5966.
[6] H. Schmidbaur, *Nature* **2001**, *413*, 31.
[7] P. Pyykkö, *Angew. Chem. Int. Ed.* **2004**, *43*, 4412.
[8] E. J. Fernández, A. Laguna, J. M. López-de-Luzuriaga, *Dalton Trans.* **2007**, 1969.
[9] E. J. Fernández, A. Laguna, J. M. López-de-Luzuriaga, M. Monge, M. Montiel, M. E. Olmos, M. Rodriguez-Castillo, *Dalton Trans.* **2009**, 7509.
[10] E. R. T. Tiekink, *Bioinorg. Chem. Appl.* **2003**, *1*, 53.
[11] E. R. T. Tiekink, J.-G. Kang, *Coord. Chem. Rev.* **2009**, *253*, 1627.
[12] E. Barreiro, J. S. Casas, M. D. Couce, A. Sánchez, J. Sordo, J. M. Varela, E. M. Vázquez-López, *Dalton Trans.* **2003**, 4754.
[13] E. Barreiro, J. S. Casas, M. D. Couce, A. Sánchez, A. Sánchez-González, J. Sordo, J. M. Varela, E. M. Vázquez-López, *J. Inorg. Biochem.* **2010**, *104*, 551.
[14] J. Chojnacki, B. Becker, A. Konitz, M. J. Potrzebowski, W. Wojnowski, *J. Chem. Soc., Dalton Trans.* **1999**, 3063.
[15] E. Barreiro, J. S. Casas, M. D. Couce, A. Sánchez, J. Sordo, J. M. Varela, E. M. Vázquez-López, *Dalton Trans.* **2005**, 1707.
[16] J. E. Huheey, E. A. Keiter, R. L. Keiter, *Inorganic Chemistry – Principles of Structure and Reactivity*, 4th ed., Harper Collins, New York, **1993**.
[17] E. J. Fernandez, A. Laguna, J. M. López-de-Luzuriaga, M. Montiel, M. E. Olmos, J. Pérez, R. C. Puelles, *Organometallics* **2006**, *25*, 4307.
[18] E. J. Fernandez, P. G. Jones, A. Laguna, J. M. López-de-Luzuriaga, M. E. Monge, M. E. Olmos, R. C. Puelles, *Organometallics* **2007**, *26*, 5931.
[19] B. Cordero, V. Gómez, A. E. Platero-Prats, M. Revés, J. Echevarría, E. Cremades, F. Barragán, S. Alvarez, *Dalton Trans.* **2008**, 2832.
[20] V. J. Catalano, A. J. Moore, *Inorg. Chem.* **2005**, *44*, 6558.
[21] V. J. Catalano, S. J. Horner, *Inorg. Chem.* **2003**, *42*, 8430.
[22] V. J. Catalano, M. A. Malwitz, A. O. Etogo, *Inorg. Chem.* **2004**, *43*, 5714.
[23] M. Contel, J. Jimenez, P. G. Jones, A. Laguna, M. Laguna, *J. Chem. Soc., Dalton Trans.* **1994**, 2515.

[24] E. Cerrada, M. Contel, A. D. Valencia, M. Laguna, T. Gelbrich, M. B. Hursthouse, *Angew. Chem. Int. Ed.* **2000**, *39*, 2353.
[25] Q.-M. Wang, Y.-A. Lee, O. Crespo, J. Deaton, Ch. Tang, H. J. Gysling, M. C. Gimeno, C. Larraz, M. D. Villacampa, A. Laguna, R. Eisenberg, *J. Am. Chem. Soc.* **2004**, *126*, 9488.
[26] Q.-H. Wei, L.-Y. Zhang, G.-O. Yin, L. X. Shi, Z. N. Chen, *J. Am. Chem. Soc.* **2004**, *126*, 9940.
[27] E. J. Fernandez, A. Laguna, J. M. López-de-Luzuriaga, M. Monge, M. Montiel, M. E. Olmos, J. Pèrez, R. C. Puelles, J. C. Sáez, *Dalton Trans.* **2005**, 1162.
[28] E. J. Fernandez, A. Laguna, J. M. López-de-Luzuriaga, M. Monge, M. E. Olmos, R. C. Puelles, *J. Phys. Chem. B* **2005**, *109*, 20652.
[29] M. Contel, J. Garrido, M. C. Gimeno, P. G. Jones, A. Laguna, M. Laguna, *Organometallics* **1996**, *15*, 4939.
[30] M. A. Rawashdeh-Omary, M. A. Omary Jr., J. P. Fackler, *Inorg. Chim. Acta* **2002**, *334*, 376.
[31] V. J. Catalano, A. O. Etogo, *J. Organomet. Chem.* **2005**, *690*, 6041.
[32] E. J. Fernandez, M. C. Gimeno, A. Laguna, J. M. López-de-Luzuriaga, M. Monge, P. Pyykkö, D. Sundholm, *J. Am. Chem. Soc.* **2000**, *122*, 7287.
[33] E. J. Fernandez, A. Laguna, J. M. López-de-Luzuriaga, M. Monge, M. Montiel, M. E. Olmos, M. Rodriguez-Castillo, *Organometallics* **2006**, *25*, 3639.
[34] A. Burini, R. Bravi Jr., J. P. Fackler, R. Galassi, T. A. Grant, M. A. Omary, B. R. Pietroni, R. J. Staples, *Inorg. Chem.* **2000**, *39*, 3158.
[35] A. Burini Jr., J. P. Fackler, R. Galassi, B. R. Pietroni, R. J. Staplers, *Chem. Commun.* **1998**, 95.
[36] E. J. Fernandez, C. Hardacre, A. Laguna, M. C. Lagunas, J. M. López-de-Luzuriaga, M. Monge, M. Montiel, M. E. Olmos, R. C. Puelles, E. Sánchez-Forcada, *Chem. Eur. J.* **2009**, *15*, 6222.
[37] K. Gajda-Schrantz, L. Nagy, E. Kurmann, A. Vertes, J. Holecek, A. Lycka, *J. Chem. Soc., Dalton Trans.* **1997**, 2201.
[38] J. S. Casas, A. Castiñeiras, M. D. Couce, N. Playá, U. Russo, A. Sánchez, J. Sordo, J. M. Varela, *J. Chem. Soc., Dalton Trans.* **1998**, 1513.
[39] H-O. Kalinowski, S. Berger, S. Braun, *Carbon-13 NMR Spectroscopy*, John Wiley & Sons, Chichester, Great Britain, **1988**, pp. 220, 233, 588.
[40] P. F. Barron, J. C. Dyason, P. C. Healy, L. M. Engelhardt, B. W. Skelton, A. H. White, *J. Chem. Soc., Dalton Trans.* **1986**, 1965.
[41] E. C. Alyea, J. Malito, J. H. Nelson, *Inorg. Chem.* **1987**, *26*, 4294.
[42] S. O. Grim, S. A. Sangokoya, A. L. Rheingold, W. McFarlane, I. J. Colquhoun, R. D. Gilardi, *Inorg. Chem.* **1991**, *30*, 2519.
[43] E. L. Muetterties, C. W. Alegranti, *J. Am. Chem. Soc.* **1972**, *94*, 6386.
[44] G. A. Ardizzoia, G. La Monica, A. Maspero, M. Moret, N. Masciocchi, *Inorg. Chem.* **1997**, *36*, 2321.
[45] L.-J. Baker, G. A. Bowmaker, D. Camp, Effendy, P. C. Healy, H. Schmidbaur, O. Steigelmann, A. H. White, *Inorg. Chem.* **1992**, *31*, 3656.
[46] S. M. Cocol, J. G. Verkade, *Inorg. Chem.* **1984**, *23*, 3487.
[47] H. Friebolin, *Basic One- and Two-Dimensional NMR Spectroscopy*, 2nd ed., VCH, Weinheim, Federal Republic of Germany, **1993**, pp. 293–297.
[48] D. Sanz, R. M. Claramunt, J. Glaser, S. Trofimenko, J. Elguero, *Magn. Reson. Chem.* **1996**, *34*, 843.
[49] D. Carmona, J. Ferrer, M. P. Lamata, L. A. Oro, H.-H. Limbach, G. Scherer, J. Elguero, M. L. Jimeno, *J. Organomet. Chem.* **1994**, *470*, 271.
[50] E. Barreiro, J. S. Casas, M. D. Couce, A. Sánchez, A. Sánchez-Gonzalez, J. Sordo, J. M. Varela, E. M. Vázquez-López, *J. Inorg. Biochem.* **2008**, *102*, 184.
[51] J. M. Perez, L. R. Kelland, E. I. Montero, F. E. Boxall, M. A. Fuertes, C. Alonso, C. Navarro-Raninger, *Mol. Pharm.* **2003**, *63*, 933.
[52] E. Barreiro, J. S. Casas, M. D. Couce, A. Sánchez, J. Sordo, J. M. Varela, E. M. Vázquez-López, *Cryst. Growth Des.* **2007**, *7*, 1964.
[53] F. C. Brown, K. Bradsher, S. G. McCallum, M. Potter, *J. Org. Chem.* **1950**, *15*, 174.
[54] Bruker Analytical Instrumentation, *SAINT: Sax Area Detector Integration*, **1996**.
[55] a) G. M. Sheldrick, *SADABS*, version 2.03, University of Göttingen, Germany, **2002**; b) G. M. Sheldrick, *Acta Crystallogr., Sect. A* **2008**, *64*, 112.
[56] A. L. Spek, *PLATON, A Multipurpose Crystallographic Tool*, Utrecht University, Utrecht, The Netherlands, **2010**.
[57] a) A. D. Becke, *J. Chem. Phys.* **1992**, *96*, 215; b) A. D. Becke, *J. Chem. Phys.* **1993**, *98*, 5648; c) C. Lee, W. Yang, R. G. Parr, *Phys. Rev. Lett.* **1998**, *B37*, 785.
[58] R. Ahlrichs, M. Bär, M. Häser, H. Horn, C. Kölmel, *Chem. Phys. Lett.* **1989**, *162*, 165.
[59] A. Schäfer, H. Horn, R. Ahlrichs, *J. Chem. Phys.* **1992**, *97*, 2571.
[60] T. H. Dunning Jr., *J. Chem. Phys.* **1994**, *100*, 5829.
[61] D. Andrae, U. Haeussermann, M. Dolg, H. Stoll, H. Preuss, *Theor. Chim. Acta* **1990**, *77*, 123.
[62] W. Kueng, E. Silber, U. Eppenberger, *Anal. Biochem.* **1989**, *182*, 16.
[63] *GraphPad Prism Software*, version 2.01, GraphPad Software, Inc., San Diego, California, **1996**.

Received: September 8, 2010
Published Online: January 27, 2011

